10

White-Light Interference 3D Microscopes

Joanna Schmit

CONTENTS

3D microscopes employing white-light interferometry (WLI) are easy to use and provide unbeatable surface topography measurements of engineered surfaces. These systems deliver vertical resolution down to a fraction of a nanometer while maintaining the submicron lateral resolution measurements found in any typical microscope.

These instruments, used both in research labs and on the production floor, are based on a digital microscope equipped with an interferometric objective (from 1× to 115× magnification) and a computer-controlled scan through focus. The precision of the height measurement, levels only possible by using the interference of light, is independent of the numerical aperture of the microscope objective and can reach vertical resolutions down to a fraction of a nanometer. A WLI 3D microscope (see Figure 10.1) functions as regular microscope but delivers height measurements at hundreds of thousands to over a million points simultaneously creating a 3D surface topography measurement.

In a single vertical scan, areas from 50 μm × 50 μm up to 20 mm × 20 mm can be measured depending on the magnification and the size of the camera chip used. The measurement

(a) (b) (c)

FIGURE 10.1
White-light interference 3D microscope (a), bifocal contact lens to be measured (b), surface measurement result of the lens (c).

is highly repeatable and reproducible, and because only light contacts the surface to be examined, no damage occurs during evaluation. Light allows for very fast and precise measurements; heights up to 10 mm are possible using commercial systems. Only the working distance of the objective limits the heights that can be measured.

This 3D surface metrology has become an established method in many industries, including the precision machining, MEMS, solar, medical, and biological fields. This method is the basis of a future ISO (International Organization for Standardization) standard for surface metrology under the name of coherence scanning interferometry (ISO/CD 25178-604). Automation of measurement including sample handling, focusing, pattern recognition data processing, and specialized analysis makes these instruments very suitable for continuous, 24-h surface topography testing with excellent gage repeatability on different surface features. Different chapters in this book discuss measurement automation in 3D microscopy.

10.1 White-Light Interference

Because the interference of light is the way that surface topography is determined, we begin with an explanation of how interference fringes are produced. White-light interferometric 3D microscopes often use Köhler illumination with superluminescent diodes (SLDs) or light-emitting diodes (LEDs) to create interference fringes around the zero optical path difference (OPD), which is set to coincide with the best focus position of the microscope. A SLD light source has a broadband visible spectrum with a bandwidth of around 100 nm. SLD combines the high power and brightness of laser diodes with the low coherence of conventional LEDs. In addition, SLDs and LEDs last a long time, consume little power, and stay relatively cool as compared to the halogen lamps previously employed in systems.

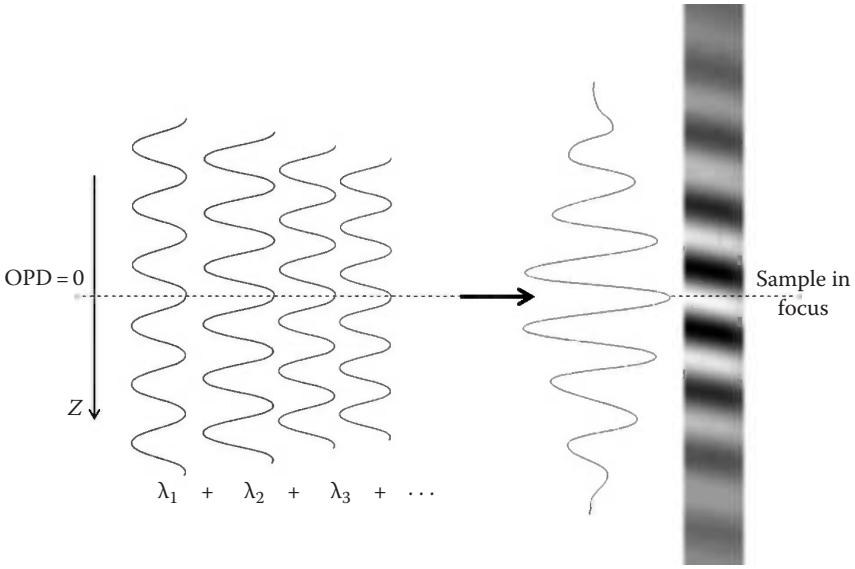

FIGURE 10.2
White-light fringe formation along axial scan *z*.

The different wavelengths λ from the source spectrum are mutually incoherent, and the superposition of interferometric fringes for individual wavelengths creates white-light fringes as shown in Figure 10.2. A solid-state CCD (charge-coupled device) or CMOS (complementary metal–oxide–semiconductor) detector observes the sum of all the fringe irradiances at each moment of the objective's scan through focus. Because each wavelength of the source creates fringes of different spacing, the maxima of fringes will align around only one point where the OPD in the interferometer is zero for all wavelengths. Away from this zero OPD position, along the axial scan z of the objective, the observed sum of the white-light fringe irradiances quickly decreases. In Figure 10.2, white-light fringes along the axial scan are presented in two ways: as a function observed by a single camera pixel, as well as grayscale image observed by a few pixels. The maximum of the fringe envelope marks the best focus position. In practice, the optical paths in an interferometer are not perfectly balanced creating slight shifts of fringes maxima.

White-light interference observed by a single pixel during an axial scan z can be mathematically described as the integral of all the fringes for all wavelengths for the full bandwidth of the spectrum and for different incident angles depending on the numerical aperture of the objective (de Groot and de Lega 2004). This summation results in the following mathematical form describing the detected fringes around the position h of the point on the object:

$$I(z) = I'\left[1 + \gamma(z)\cos(k_0(h - z) + \varphi)\right] \tag{10.1}$$

where

I' is the background irradiance
$\gamma(z)$ is the fringe visibility function or coherence envelope along axial scan z
$k_0 = 2\pi/\lambda_0$ is the central wave number for fringes under the envelope
φ is the phase offset of fringes maximum from the envelope's maximum due to dispersion in system

The broader the bandwidth of the source spectrum, the narrower is the width of the envelope. For a white-light source, this width is on the order of 1–2 μm. Determining the position of each of the envelopes on each point on the object is equivalent to finding the best focus position *h*-*z* at each point with great precision due to the narrowness of the envelope of the fringes. Best focus position at each point in turn determines the object's topography.

10.2 Measurement Procedure

The measurement procedure is simple, and no special sample preparation is needed. The sample is first placed underneath the objective. Then the sample needs to be brought into focus by moving either the objective or the sample plus its stage vertically as with regular optical microscopes, the main difference being that on portions of the sample which are in focus a few fringes will appear. Then the top or the bottom of the surface may need to be found manually or automatically by bringing it to focus. Once found, measurement can begin. The automatic scan will bring the sample beyond the focus and then scan the sample through its desired height while a camera will be collecting images at constant rate. The images will include fringes required for the topography measurement with this method. A scan has to start from the position at least a few microns above the highest point on the surface to be measured to a few microns below the lowest point to be measured; thus, a scan starts and ends with no fringes in the field of view.

Figure 10.3 presents four camera frames with interferograms from a scan through focus for a semispherical surface. Each interferogram shows the part of the object that is in focus for a given scan position.

The shape of these fringes already provides information about the spherical topography of the object. Additionally, a grayscale image of the fringe signal as seen by a few pixels during scan through focus is shown under the objective in Figure 10.3. For mirrorlike surfaces without steps or scratches, only these fringes are signaling when the sample is in the best focus position since no other object features "come to focus." Thus, 3D white-light interferometric microscopes are ideal for measuring smooth, mirrorlike finished surfaces.

Measurement of the best fringe contrast position results in a nanometer level precise measurement of surface topography. Methods for finding the position of best contrast fringes were described by many authors (Ai and Novak 1997, Caber 1993, Danielson and Boisrobert 1991, de Groot and Deck 1995, Kino and Chim 1990, Larkin 1996, Park and Kim 2000).

Unlike the monochromatic interferometric techniques, white-light interferometric techniques can be used for measuring not only smooth but also rough surfaces. Applications for this technique are enormously varied; for example, surface roughness that affects the cosmetic appearance of glossy paper or car finishes can be measured including the food roughness which apparently affects our eating experience. But 3D profilers are also commonly used to measure roughness of engine components, other machined parts (see Figure 10.4), bearings, or medical implants and contact lenses for which roughness and its character determines functionality of the part.

White-light fringes for rough surfaces can vary from locally well-defined fringes to fringes in the form of speckles. Figure 10.5 shows four through-focus images for a rough sample. Two images taken from above and below the sample's height range show no fringes, and two images taken at two different focus positions on the sample show clear fringes. The fringes indicate rather smooth islands along with rougher valleys among the islands.

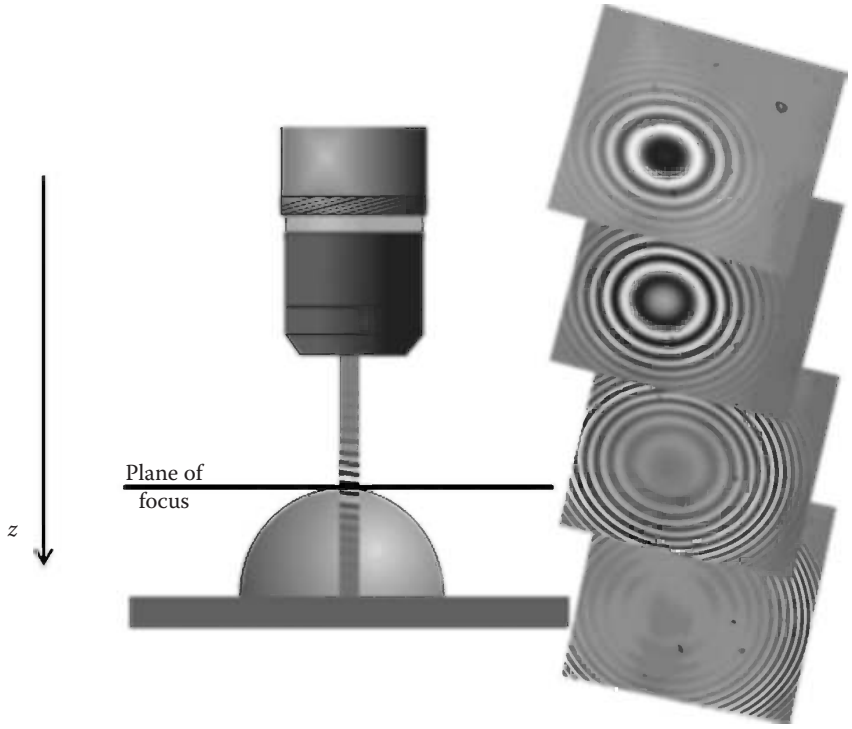

FIGURE 10.3
Four interferograms from a scan through focus for a semispherical surface.

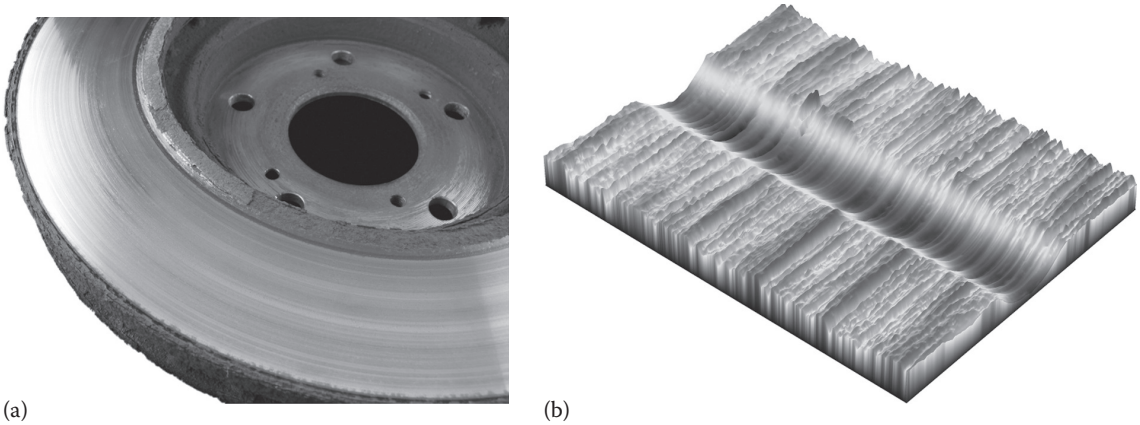

(a) (b)

FIGURE 10.4
A metal machined part (a) and the measurement result of wear mark on this part (b).

10.3 Interferometric Objectives

3D WLI microscopes use interferometric objectives that are based on infinity-corrected bright-field objectives with a beam splitter and a reference mirror. The interferometer portion enhances determination of the focus position by creating fringes around the best focus allowing for object shape measurement with sub-nanometer resolution for high as well

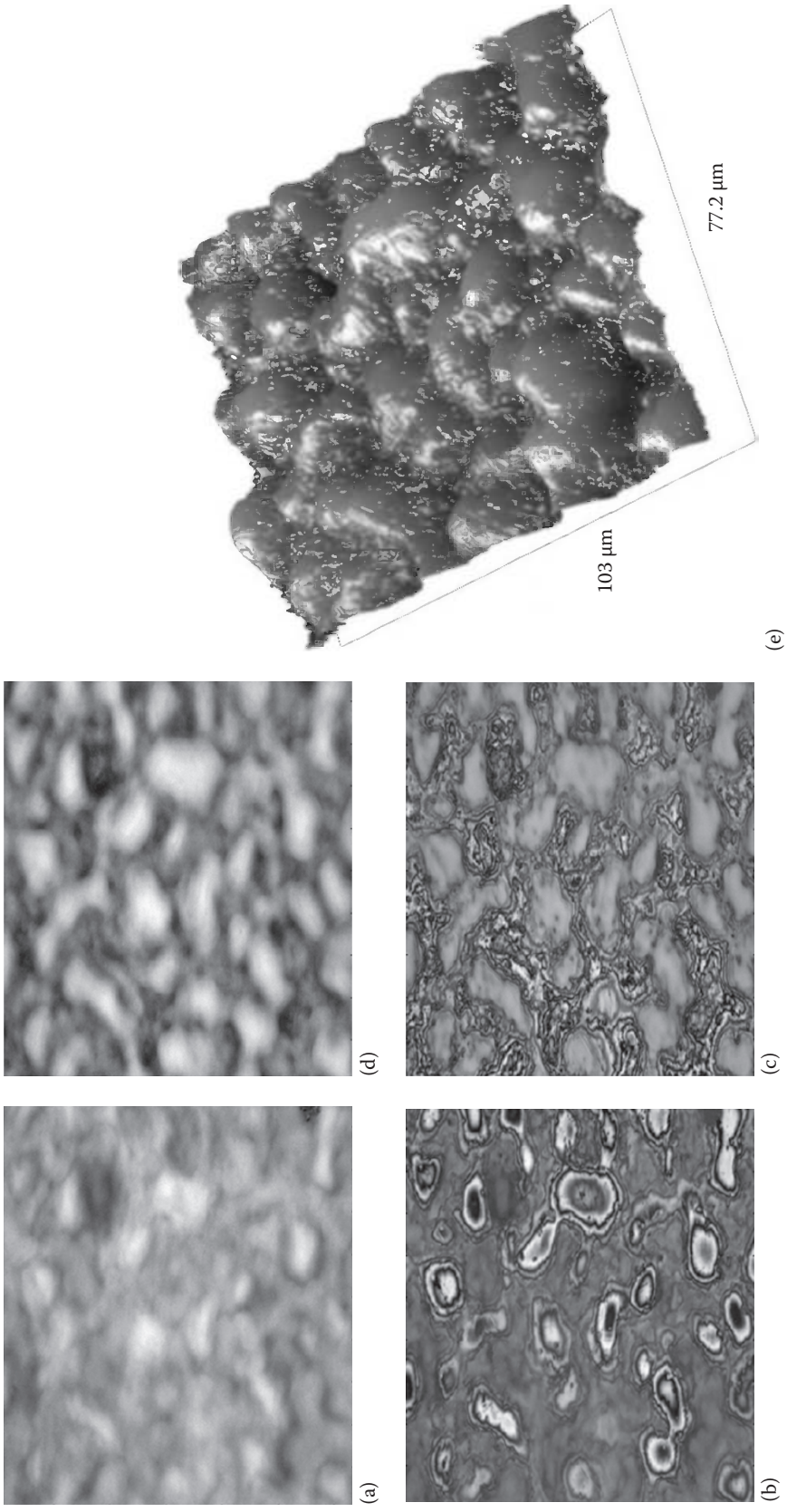

FIGURE 10.5
3D WLI microscope images for rough surface taken (a) above and (d) below the sample height range that show no fringes. (b) and (c) show two different focus positions on the sample and show fringes. (e) is the measurement result with average roughness Ra = 419 nm.

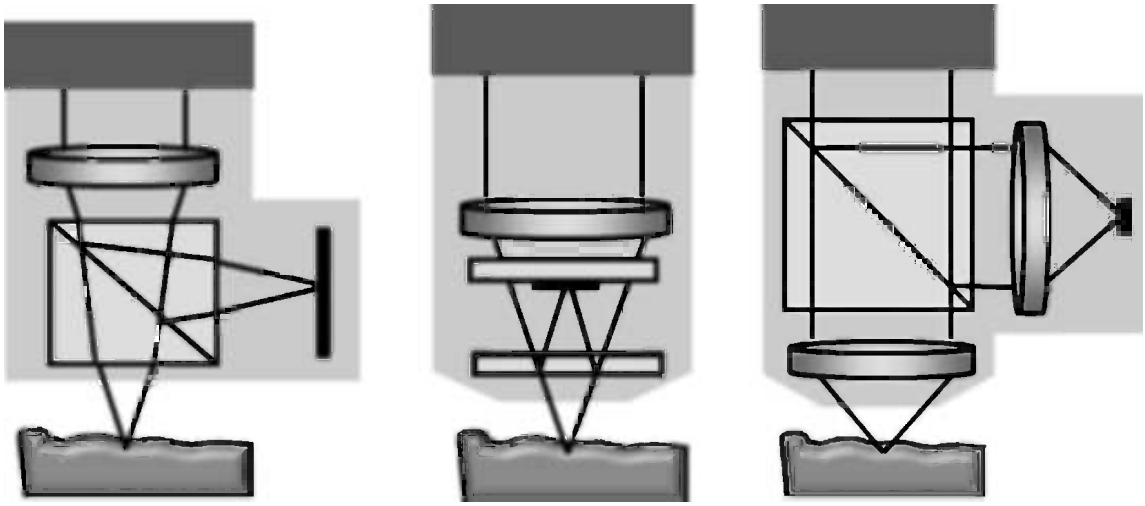

FIGURE 10.6
Interferometric objectives: (a) Michelson (b) Mirau and (c) Linnik.

as low magnification. Three basic interferometric objectives are used in these systems: Michelson, Mirau, and Linnik.

A Michelson interferometric objective uses a beam splitter cube placed underneath the objective and a reference mirror placed to the side (see Figure 10.6a); this type of interferometer is used only with low-magnification objectives having a long working distance and thus low numerical apertures. The Mirau interferometric objective (Figure 10.6b) uses two thin glass plates underneath the objective in objectives with shorter working distances and thus medium to high magnifications. The lower plate acts as a beam splitter, and the plate above contains a small reflective spot that acts as the reference surface. Mirau setups are not very useful at magnifications of less than about 10× because at these lower magnifications, the reference spot needs to be bigger as the field of view gets bigger, and then spot obscures too much of the aperture.

The third type of interferometric objective, a Linnik objective, is built for a few different reasons. The Linnik system (Figure 10.6c) allows an interferometer to be set up for any magnification objective from two identical bright-field objectives and beam splitter before objectives. Thus, such objectives can be built in the lab for any magnification. On one hand, the Linnik systems may be the only solution for very high-magnification, high-numerical aperture objectives that have short working distances that could not facilitate a beam splitter plate. On the other hand, the Linnik objective may be the only solution if a long working distance needs to be maintained for the measurement of large samples.

However, these objectives are quite bulky, and for higher magnifications, they may be very difficult to adjust since not only the position of the reference mirror needs to be adjusted but also the position of the objective and the reference mirror separately. In addition, the two objectives need to be matched with a beam splitter to provide a wavefront with minimum aberration and maximum fringe contrast.

10.3.1 Alignment of Interferometric Objectives

In order to obtain fringes at best focus, the position of the reference mirror needs to be set also at the best focus of the objective. This is done in three steps (see Figure 10.7): first, the

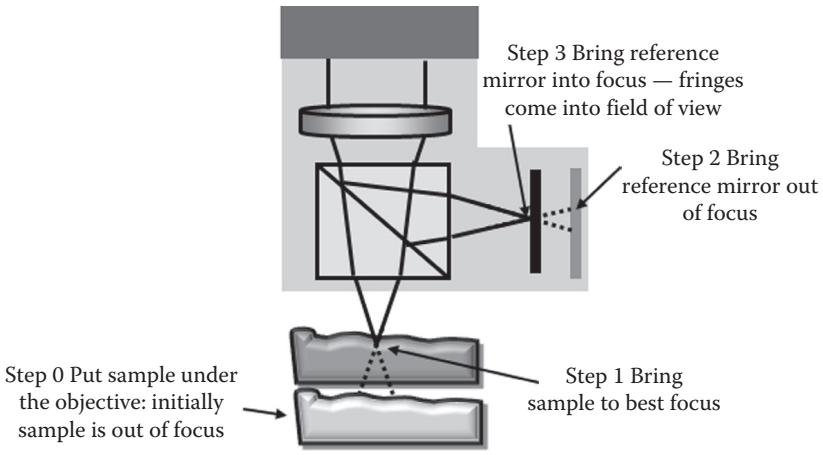

FIGURE 10.7
Procedure of interferometric objective alignment.

reference mirror is moved a few or tens of microns away from focus; second, the objective is focused on the object with some features like the edge of a sharp but not too tall step (fringes are not visible at this moment); and third, the reference mirror is brought to focus and stopped when best contrast fringes are obtained. When best contrast fringes and best sample focus are achieved, the zero OPD between arms of the interferometer coincides with best focus. This procedure is done in the factory, and the position of the reference mirror is then locked before shipping the system.

10.4 Calibration of WLI 3D Microscope

In order to provide precise and accurate measurements of surface topography, each microscope needs to be calibrated not only in the lateral but also vertical dimensions. Calibration is commonly done using special "artifacts" with certified heights and lateral features. Calibration artifacts need to be handled with care and stored and cleaned in accordance with manufacturer's instructions.

10.4.1 Lateral Calibration

Lateral calibration in x and y direction serves as a magnification calibration and is done for each objective and field of view lens. A calibrated pattern on the artifact is measured, and its lateral scale is set to match the lateral size of features via a magnification value setting. The pattern may be a grating composed of parallel lines or concentric circles.

Nowadays, systems are designed for the infinity-corrected objectives. It is worth noting that the magnification of the objective is not the value assigned to the objective but the combination of objective and the microscope's tube length. The tube length may vary between 160 and 210 millimeters, and thus, if the nominal magnification of the objective assigned by the manufacturer is based on a 160 mm tube length, then the magnification of this objective on a system with 210 mm tube length will be about 30% greater, as magnification equals tube length divided by the focal length of the objective.

10.4.2 Vertical Calibration

The vertical calibration relies on the proper settings of scanner speed, the cameras collected number of frames per second, and the known distance the scanner has traveled. This distance may be determined by the height of a calibrated artifact or by the interference fringes of a stable source wavelength.

Typically, such calibration is done via the measurement of a known step-height standard (SHS). Calibration is done by means of changing the scanner speed to achieve the value of the NIST (National Institute of Standards and Technology) or PTB (Physikalisch-Technische Bundesanstalt) traceable artifact to be within its allowable determined uncertainties. These standards are called secondary standards because their value is measured against a primary step-height standard established by NIST or PTB. Step-height standards come in different heights from nanometer through micron ranges. This type of calibration determines the average scanner speed and assumes that the scanner's speed remains constant both over the whole range of the scanner and across many measurements. For faster measurement of tall samples, scanner speed can be set even to approximately 100 μm/s (Deck and de Groot 1994, Schmit 2003). Often, the overall variations in scanner performance are mapped at the factory and corrected, but this correction may not remain stable over time.

Because of the number of possible different sources of uncertainty such as scanner inconsistency, nonlinearities, ambient temperature changes, and variances in secondary standard values, a primary standard can be embedded into WLI 3D microscopes that evaluates each moment of every measurement and continuously self-calibrates the system for maximum precision (Olszak and Schmit 2003). The primary standard is based on the wavelength of an additional embedded laser interferometer, which continuously monitors scanner motion, measures the wavelength of the detected fringes, or gives a trigger signal to collect images at constant distances. The repeatability of step-height measurement can be achieved on the order of only a few nanometers over a long period of time (days) and regardless of the changes in ambient temperature.

The need to rapidly inspect components by white-light interferometry has become increasingly important especially for high-volume manufacturing environments. For example, data storage firms use multiple machines continuously to screen hundreds or thousands of magnetic heads per hour in a reliable, automated way with a minimum of user control. In situations where multiple machines measure the same parts with sub-angstrom precision, repeatability and system to system correlation play a crucial role in production. In these cases, not only must the same measuring procedure and analysis be applied across all the systems but also the alignment and calibration of the systems must be well established and controlled.

10.5 WLI 3D Microscope Settings and Surface Properties to Be Measured

In order to correctly measure the sample's surface over the area, one has to have a strong knowledge of the system's abilities and limitations as well as the properties of the surfaces to be measured in order to assess if the system will be acceptable for the required measurement.

There is a wide range of options available when it comes to 3D measurement systems, but systems based on microscopes will most likely be best for measuring objects with

small features, and an interferometric method of measurement is highly desirable for its unparalleled vertical precision and measurement speed. In other words, a WLI 3D microscope will be the best choice when roughness measurements, lateral resolution, vertical precision, and speed are important. When only form needs to be measured and lateral resolution larger than 10 μm is sufficient, then other methods not based on the WLI microscope should be considered.

Once the WLI 3D microscope has been chosen as the measurement instrument, one will have to make some decisions within the system. For example, the choice of objective will depend on the size of the total area to be measured and the lateral features, roughness, as well as the angle of local smooth slopes. While the magnification of the objective (plus intermediate optics and tube length) and size of the CCD camera determine the measurable area, the numerical aperture (NA) of the objective determines what lateral features on the object can be measured and the maximum measurable smooth slopes. In this section, we discuss a wide range of sample features that can be successfully measured with a white-light interferometric microscope. In addition, we discuss if the presence of film and dissimilar materials on the sample, or even the cover glass above the sample, will require some special consideration and solutions.

10.5.1 Vertical Size

We often think of microscopes as examining very small samples, a smear of blood on a glass slide slipped under the aperture like in high school biology. However, nowadays, small features needing measurement are often part of much larger systems. In these cases, the setup of the microscope needs to be much more flexible. One solution is to mount the WLI 3D microscope on a large frame platform, so the sample can fit under the objective; alternately, the WLI 3D microscope must be designed to be portable so that it can be brought to large samples like printer rollers or engines. These systems also require the ability to tilt at large angles so that the objective is roughly perpendicular to the surface as shown in Figure 10.8.

10.5.2 Vertical Resolution

Samples that require high-precision measurement should be tested using an interferometric technique because of this method's ability to deliver results with nanometer or a fraction of a nanometer vertical resolution. Interferometric objectives, in contrast to methods based on bright-field objectives, deliver excellent vertical resolution regardless of their magnification (numerical aperture).

The quality of the vertical measurement with bright field objectives will vary depending on the numerical aperture/magnification of the objective. The precise measurements can only be achieved using the highest, 50× or 100×, magnifications since only for these objectives is a very small portion of object imaged with sharp focus. Clearly, different parts of the object will come into focus with the vertical motion of the objective providing the information to make a measurement. These high-magnification bright-field objectives have a small depth of field on the order of a few microns. For low-magnification objectives, 5× magnification, for example, the whole sample may be in sharp focus at once. In this case, determining the best focus plane is impossible because of the large depth of field.

The quality of the vertical measurement with interferometric objectives is determined by the width of the fringe envelope and not the depth of field of the objective. The width of the fringe envelope, which is based on the bandwidth of the light source, typically on the

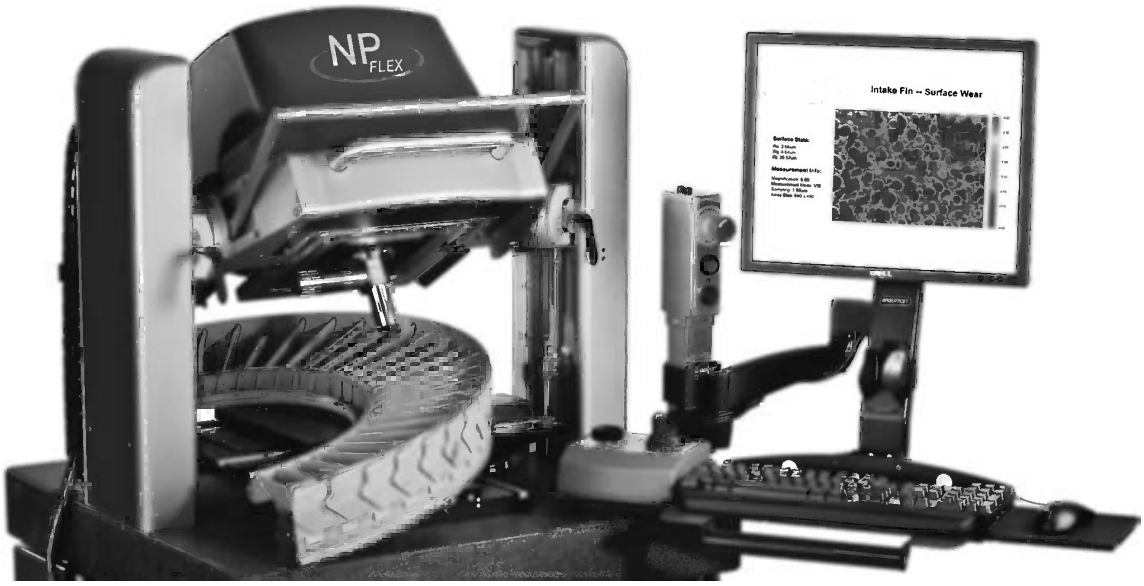

FIGURE 10.8
WLI 3D microscope system on large platform adapted to the measurement of significantly titled surfaces on large objects.

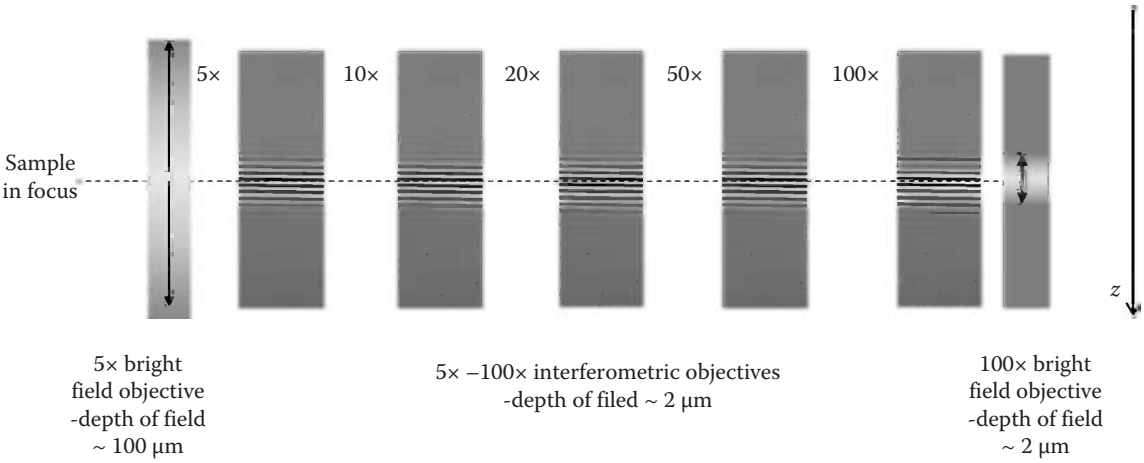

FIGURE 10.9
White-light fringe envelope spans a few microns around the best focus for any magnification objective, while the depth of field of non-interferometric objectives can be as large as 100 μm for 5× magnification and only can go down to a few microns for the highest magnifications.

order of 1–2 μm, is the same for any objective as shown in Figure 10.9; this allows for the same great height precision measurements regardless of the objective.

Nanometer and sub-nanometer level measurement precision requires stable environmental conditions; an anti-vibration air table is required to achieve optimal precision. The low noise of the measurement allows for the excellent vertical resolution but creates some susceptibility to vibrations in the form of ripples following the fringes. Non-interferometric measurements typically have a noise level that is higher than the level of ripples coming from vibrations, and thus, these ripples are not noticeable in the measurement noise of non-interferometric systems but at a cost of vertical resolution.

With white-light interferometric methods, sub-nanometer vertical resolution can be achieved but only for smooth, close to mirrorlike quality surfaces. For these smooth surfaces, the phase of the fringe maximum carries information about object height; measuring this phase position enables the sub-nanometer precision. For stepped, smooth surfaces in addition to measuring the envelope peak, the phase of fringes can also be measured (de Groot et al. 2002, Harasaki et al. 2000); this allows for the measurement of tens of microns tall steps and at the same time sub-nanometer level measurement on step surfaces. Figure 10.10 shows an example of locally smooth surface measurement, first with fringe envelope peak detection and then with combined fringe envelope and phase detection. Measured roughness from a few nanometers reduces to a fraction of nanometers. Figure 10.11 shows the result of 4 nm tall binary grating measured with a 20× objective and a fringe envelope peak and phase detection method. The noise level of this method easily allows for the measurement of a single nanometer tall grating.

Rougher surfaces (above roughness Ra = 50 nm) can only be measured using peak envelope position because the phase information loses its meaning on these rough surfaces (Dresdel et al. 1992). Measurement of optically smooth surfaces (roughness Ra below 20 nm) may be

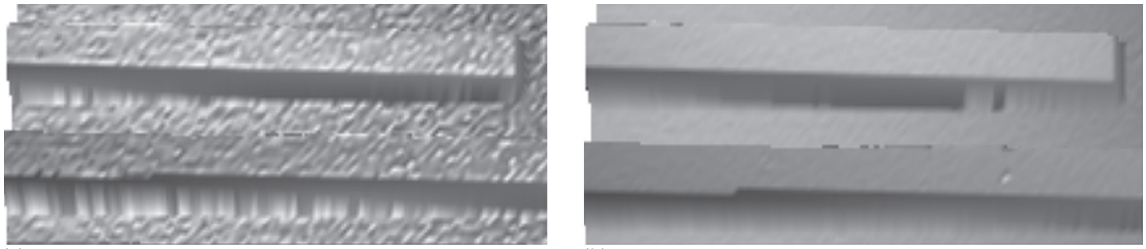

FIGURE 10.10
Surface roughness of smooth surface calculated with algorithm based on (a) fringe envelope peak detection and (b) combined fringe envelope peak and phase detection.

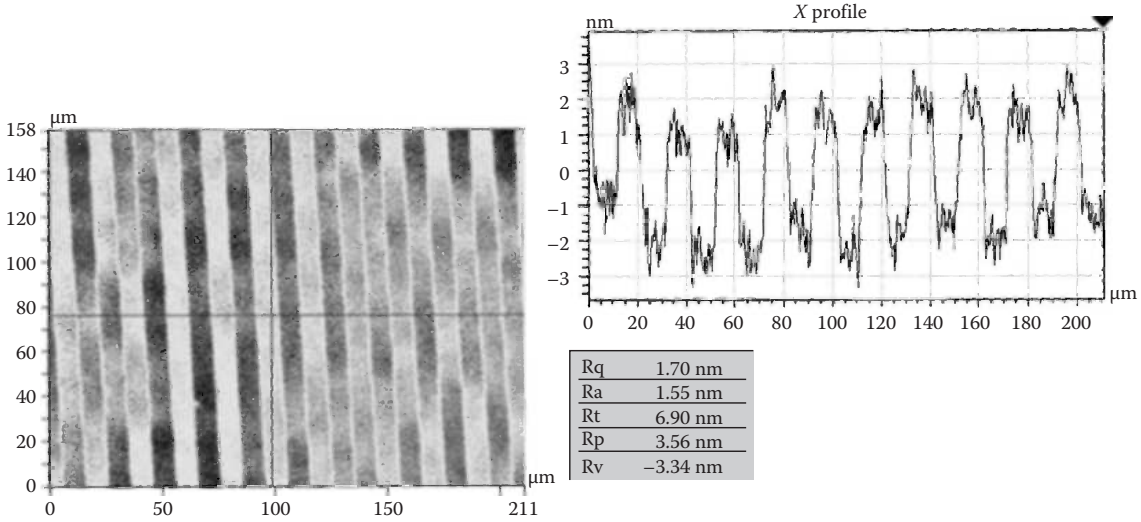

FIGURE 10.11
Four nm tall binary grating measured using a fringe envelope peak and phase detection method that yields results sub-nanometer vertical resolution (meaning very low noise).

based only on the phase of the fringes; this method is called phase shifting interferometry (PSI) and does not require fringes with decreasing amplitude of the envelope. However, the limitation of PSI is that only objects that have discontinuities less than about quarter of the wavelength (typically around 150 nm) can be measured. A significant advantage of PSI is that measurement time is only on the order of a fraction of a second and vertical resolution easily reaches sub-angstroms. Many article and book chapters have been written on phase shifting interferometry (i.e., Schreiber and Bruning 2007)

10.5.3 Lateral Size

The size of the measured area depends on the magnification of the system and the camera. In general, objectives of lower magnification can measure samples up to 20 mm × 20 mm, while the highest magnifications (100× objective) have fields of view of about 50 μm × 50 μm. A stitching procedure based on multiple measurements with a slight lateral overlap allows for the measurement of larger areas. Often, the stitching procedure is used if a high-magnification objective is required to resolve high slopes and small lateral features on the sample and larger areas also need to be measured. Figure 10.12 shows the measurement of roughly a 25 mm diameter Arizona quarter coin measured with a 5 mm field of view objective. Profiles show height changes from which lateral dimensions can be measured.

10.5.4 Lateral Resolution

Optical resolution determines the resolvable size of the lateral features on the object. This resolution depends only on the wavelength and the numerical aperture of the microscope objective and ranges from a few microns to a fraction of a micron for higher magnification objectives. Sparrow and Rayleigh (Born and Wolf 1975) cite slightly different criteria for an incoherent system imaging two radiating points as an object:

$$\text{Sparrow optical resolution criteria} = \frac{0.5 * \lambda}{\text{NA}} \tag{10.2}$$

$$\text{Rayleigh optical resolution criteria} = \frac{0.6 * \lambda}{\text{NA}} \tag{10.3}$$

Although these criteria are a good approximation for a WLI microscope, we have to remember that two lines can be better distinguished than two points, and for the WLI 3D microscope, height changes also influence the lateral resolution (de Groot and de Lega 2006). In addition, registering an image with a CCD camera requires at least three pixels in order to resolve an image of two points. Systems with low-magnification objectives may be limited by detector sampling. Thus, lateral resolution will depend on the larger of the optical resolution and the lateral sampling of the detector. Typically, microscope systems are optically limited for magnifications 20× and higher and detector limited for magnifications 5× and lower. Lateral resolution beyond the diffraction limits is difficult but possible to achieve on systems with sub-nanometer vertical resolution, an excellent scanner, and good knowledge of the system applied in the algorithm. Images in Figure 10.13 show the improvement in lateral resolution beyond the diffraction limits of 200 nm period grating, measured with an enhanced surface interferometric system and algorithm, over the

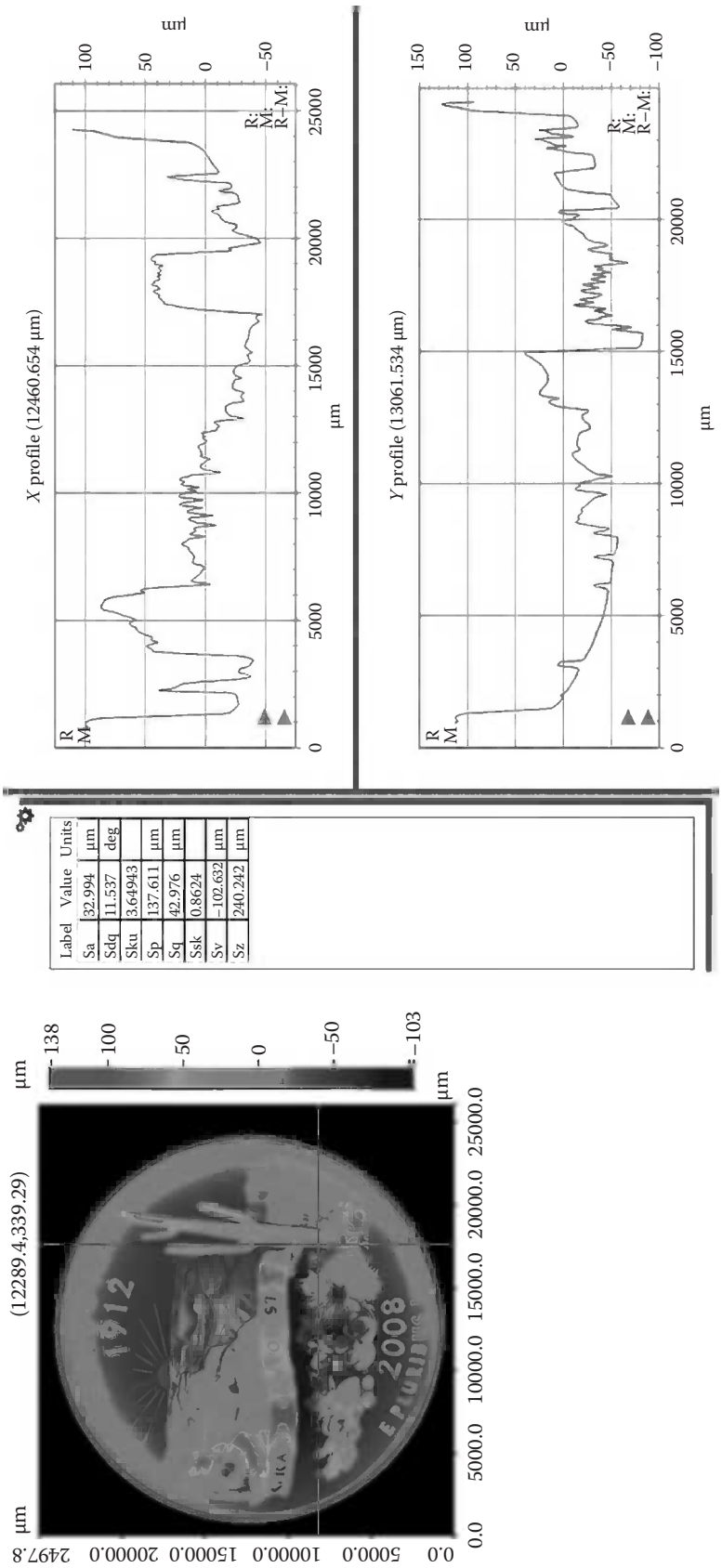

FIGURE 10.12
Topography of Arizona quarter coin measurement including two profile traces.

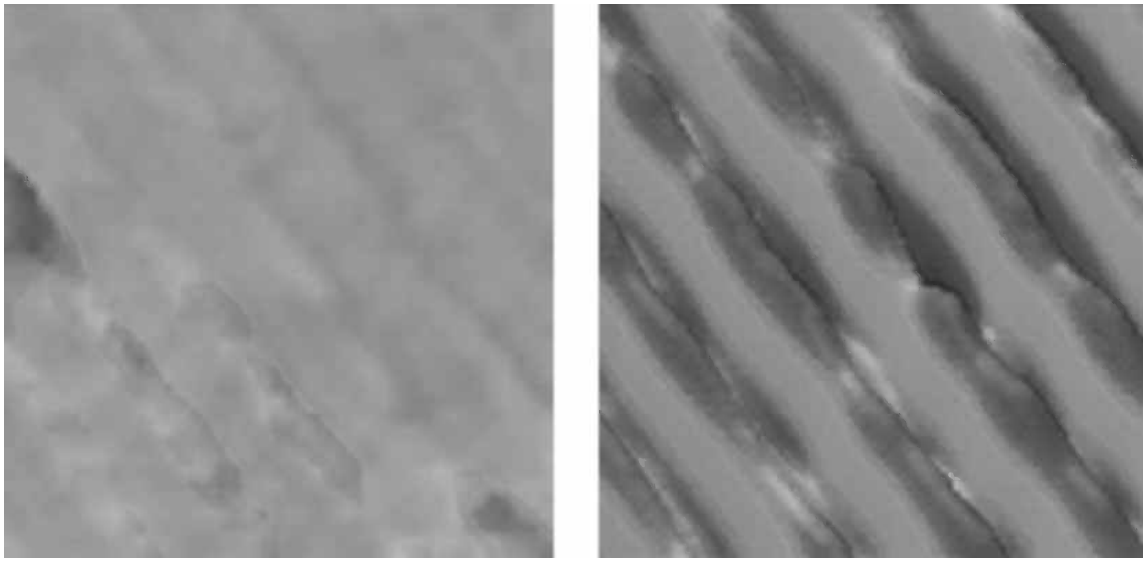

(a) (b)

FIGURE 10.13
Two hundred nanometer period binary grating as measured using (a) white-light interferometric measurement resulting in hardly resolvable features and (b) enhanced interferometric measurement with improved lateral resolution.

regular measurement (Novak and Munteanu 2011). Excellent vertical and lateral resolution allows for measurement of fine structures as well as small defects and scratches on solar cells, plastic films, and any other high-quality surfaces.

10.5.5 Lateral Dimensions

With information about object height, it is easy to distinguish, for example, traces, and automatically determine their widths, lengths, and distances as shown in Figure 10.14. In order to improve the precision of the measurement, the height map of each sample can be aligned to the same orientation, which makes measuring the x and y dimensions easy and repeatable. Lateral and vertical dimensions along with other parameters like curvature or roughness can be calculated for each of the identified features on the object.

10.5.6 Surface Slopes

Surface topography refers to the different heights, slopes, and roughness present on a sample. Regardless of the sample topography, light must come back to the objective in order for the surface features to be measured. The amount of light gathered by the objective depends on its NA. The limits on the maximum measurable slope differ depending on whether the surface being measured is smooth or rough. A smooth, mirrorlike sloped surface reflects light in mainly one direction according to the specular reflection angle, while a rough surface reflects light in a range of directions dependent on the specific properties of the surface. As shown in Figure 10.15, if light that is reflected from the sloped smooth surface totally misses the objective, the slope cannot be measured. However, some light that is reflected from a similarly sloped but rough surface will make its way to the objective and measurement of the overall shape and slope is easy.

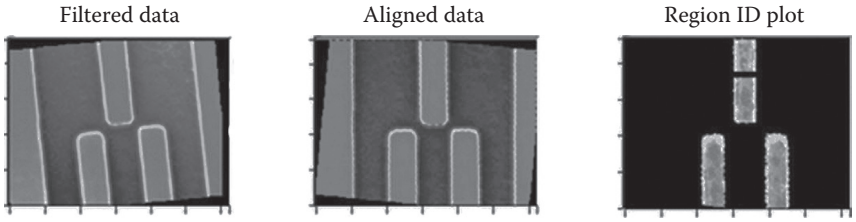

Height		Lateral	
Very top avg height	381.62 nm	Very top Y width	4.35 μm
Top avg height	385.11 nm	Very top X width	2.98 μm
Left avg height	386.08 nm	Top Y width	6.32 μm
Right avg height	382.96 nm	Top X width	3.03 μm
		Left X width	3.09 μm
		Left Y width	9.89 μm
		Right Y width	10.21 μm
		Right X width	3.06 μm

FIGURE 10.14
Measured traces before and after rotational alignment and with identified traces regions and their vertical and lateral parameters calculated.

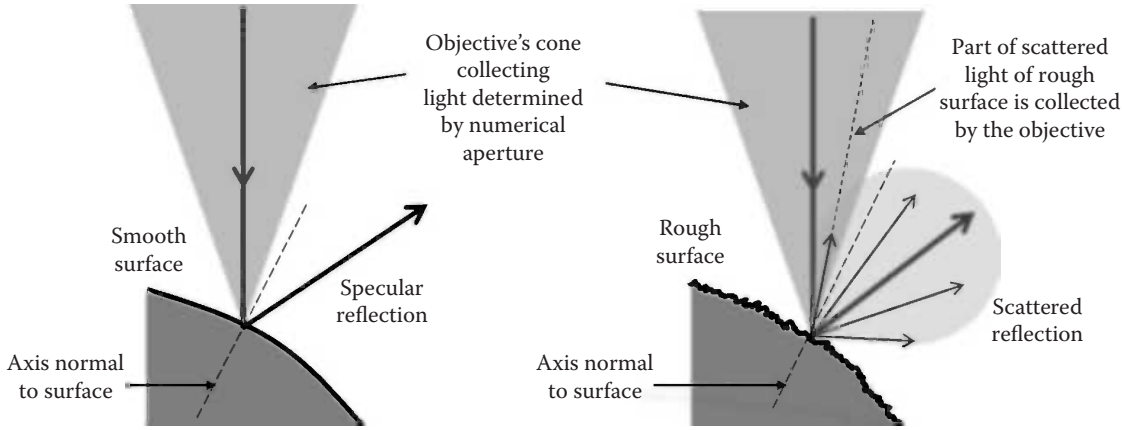

FIGURE 10.15
Scattered light reflecting from a rough surface allows for the measurement of higher slopes.

The common maximum NA for an interferometric objective is about 0.8 for magnifications 50–115× objectives. With this NA, smooth slopes up to 35° can be measured. Thus, a wide range of microlenses, Fresnel lenses, solar cells, and patterned sapphire structures for LED manufacturing can be successfully measured (see Figure 10.16).

In addition, objects with rough surfaces and higher slopes (up to 60°–70°) like some holographic films and woven materials can also be measured since rough surfaces allow some light to travel back to the objective.

WLI 3D microscopes for engineered surfaces must account for the fact that the sample often is not flat and may have surfaces at different angles. For this reason, the sample needs to be placed on a stage that can be tilted. Alternately, the objective can be tipped and tilted around the sample to accommodate the surface angles. During the relative tip and

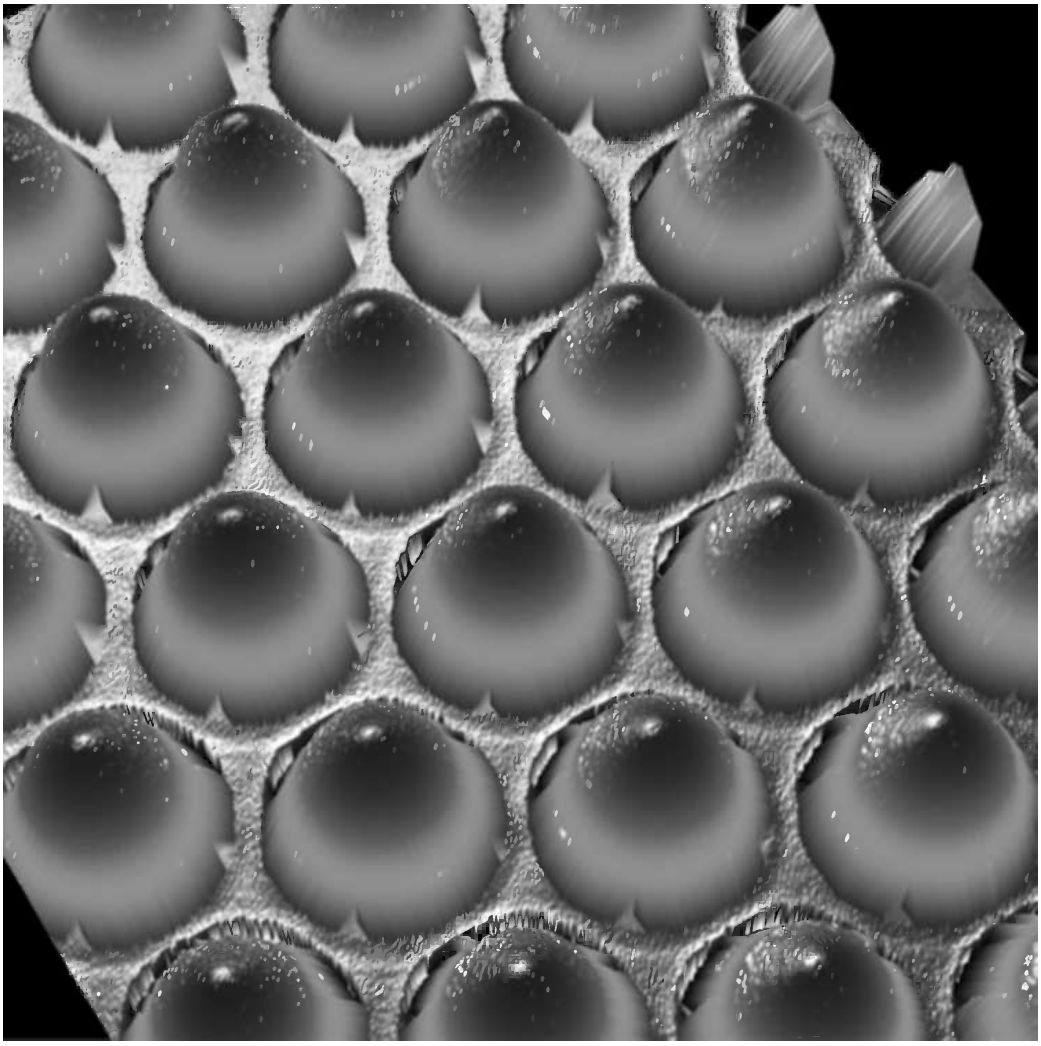

FIGURE 10.16
Patterned sapphire structure with elements about 3 µm tall and 1.5 µm wide measured with 115×, 0.8 NA objective using a special combination of fringe envelope and phase detection. Results agree very well with atomic force microscopy measurement.

tilt between the objective and sample, fringes will change density and shape as shown in Figure 10.17. For best measurement results with low noise, dense fringes should be avoided, which can often be done by changing the tip or tilt.

10.5.7 Dissimilar Materials

As long as the object's surface is comprised of a single material, the light has a consistent phase shift per wavelength upon reflection. However, when two dissimilar materials are side-by-side on the surface, they will have different phase shifts Φ upon reflection for different wavelengths (unless both of them are dielectric materials with the imaginary part of the index of refraction $k = 0$ and thus transparent), and the measured height difference at the boundary where the two meet will be incorrect (Doi et al. 1997). This difficulty can be overcome by knowing the optical constants of the different materials

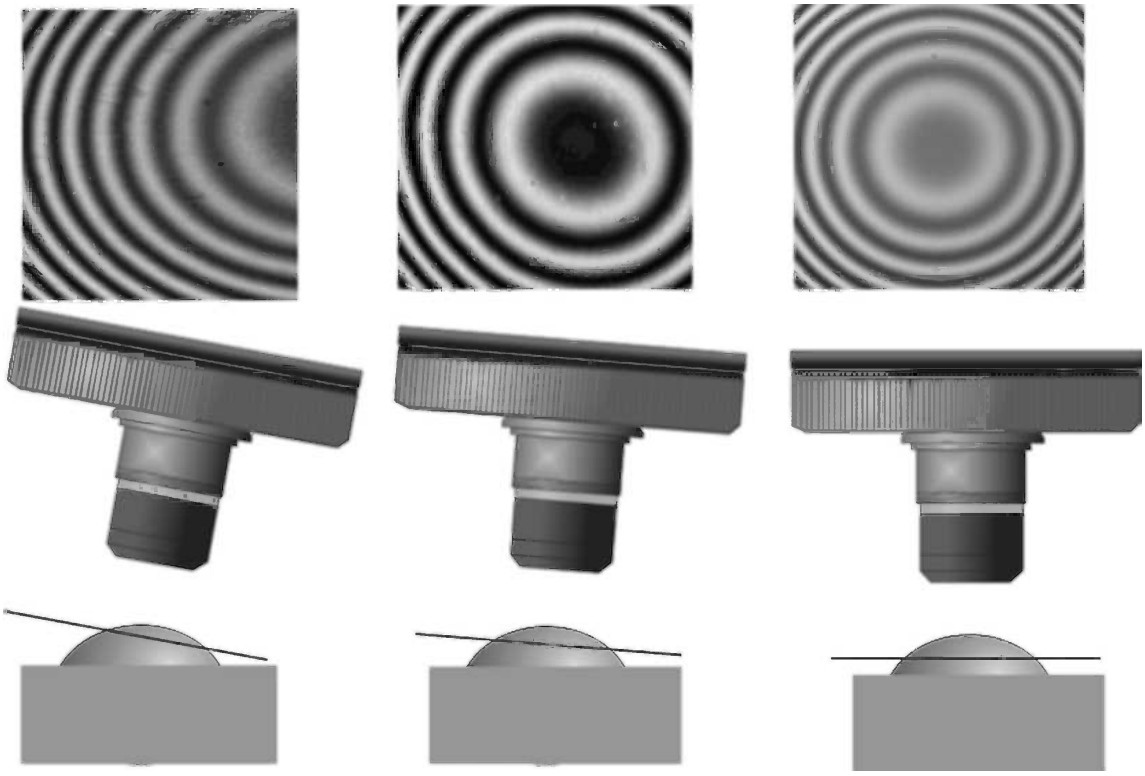

FIGURE 10.17
Tilt of interferometric objective with respect to sample changes the fringe frequency, shape, and direction. Tilt can be adjusted for better measurement of sloped surface.

for the wavelengths used in the measurement and correcting for this difference. Using monochromatic illumination, which has only single values for n and k, makes this calculation easier because the height difference can be calculated from the following equations (Born and Wolf 1975):

$$\Phi(n,k) = \arctan\left(\frac{2k}{1-k^2-n^2}\right) \tag{10.4}$$

$$\Delta h = \frac{\lambda}{4\pi}\Delta\Phi = \frac{\lambda}{4\pi}\left[\Phi\left(n_1,k_1\right) - \Phi\left(n_2,k_2\right)\right] \tag{10.5}$$

Figure 10.18 shows the phase change upon reflection effect on a plane wavefront incident on a flat sample made of two different materials.

In white-light interferometry, different materials that make up the sample will shift the peak of the envelope (metals more so than other materials) and possibly even change the shape of the envelope (for example, gold and some semiconductors). However, for most materials, this shift will not be larger than 40 nm (Harasaki et al. 2001, Park and Kim 2001). For example, a trace made of silver on glass will appear about 36 nm taller and aluminum about 13 nm taller. These offsets often may be negligible for the measurement and can be disregarded completely.

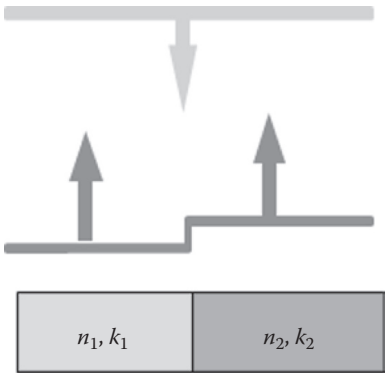

FIGURE 10.18
The phase of the wavefront reflected off materials with different n and k complex indices of refraction may be different for each material and must be accounted for when measuring surface height.

Apart from accounting for different phase shifts using constants, several alternate ways to achieve accurate measurements exist. The phase shifts can be determined by comparing the WLI result to a contact measurement like a stylus profiler (Schmit et al. 2007) and subsequently compensate for the shifts in the algorithm. Additionally, the sample may be coated with a nontransparent 100 nm layer of gold and then measured with the 3D microscope before and after coating to determine the shift. Finally, a mold of the area using silicon rubber can be used to create a replica of the sample. This replication method is also useful when the sample cannot be brought to the microscope.

10.5.8 Thick Film Measurement

If the sample is covered with a transparent film that is more than a few microns thick, two sets of localized fringes separated from each other are generated, one for each interface as shown in Figure 10.19. However, fringes for the second interface are localized below this interface by roughly half of the product of the group index of refraction for white light and the geometrical thickness of the film. A simple technique for finding the relative position

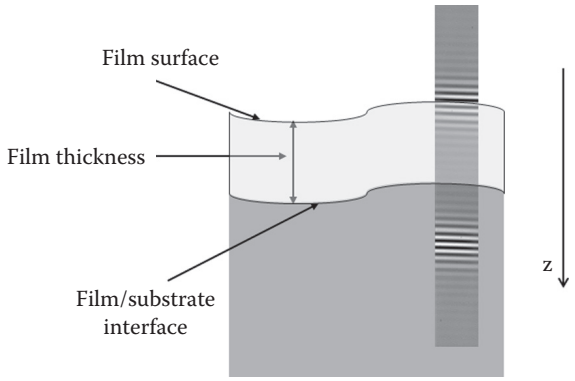

FIGURE 10.19
White-light fringes for a few micron transparent films with emphasis that the film thickness as well as its top and bottom topography can be measured.

of the peaks of the fringe envelopes can be implemented to find the thickness of the film as well as topography of the top surface and interface.

The typical range of measurable film thicknesses runs from 2 to 150 μm depending on the dispersion of the film and the NA of the objective. Typically, one sigma of repeatability for a film thickness measurement is about 6 nm. For the measurement of thicker films, objectives with lower NAs as well as illumination spectrums narrower than white light should be used to improve the contrast of fringes from the film-substrate interface. For the measurement of thinner films, a full spectrum of white light should be utilized, and a higher numerical aperture objective may be helpful. Of course it is possible to measure the thicknesses of individual layers in multiple layer coatings as long as the fringes for each layer are detected and separated. White-light fringes will also be created at defects; thus, this method can also be used for detection and localization of defects in films.

10.5.9 Measurement through the Glass Plate or Liquid Media

Some products need to be tested in their final stage, which often means the testing occurs through a protective liquid, plastic, or glass. Many engineering objects, like MEMS devices, are protected by a cover glass, and some devices in environmental chambers need to be tested under different pressures or temperatures. Biological and some mechanical samples are often immersed in liquid and require measurement through this liquid (Reed et al. 2008a,b). Because of the dispersion of the liquid, plastic, or glass, the white-light fringes may be totally washed out (see Figure 10.20). For this reason, a compensating plate needs to be placed into the reference arm of interferometer. This compensation is the most easily done for Michelson (see Figure 10.21) and Linnik-type objectives; however, compensating plates for Mirau-type objectives also exist. Compensating plates also can help with measurements of thick films as well as samples in liquid.

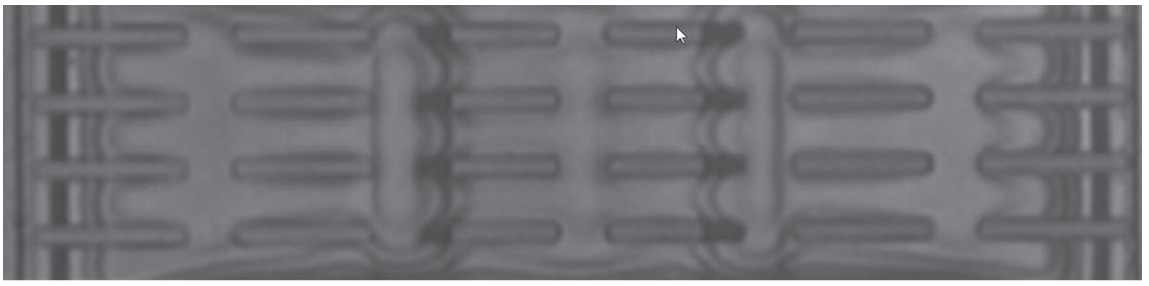

(a)

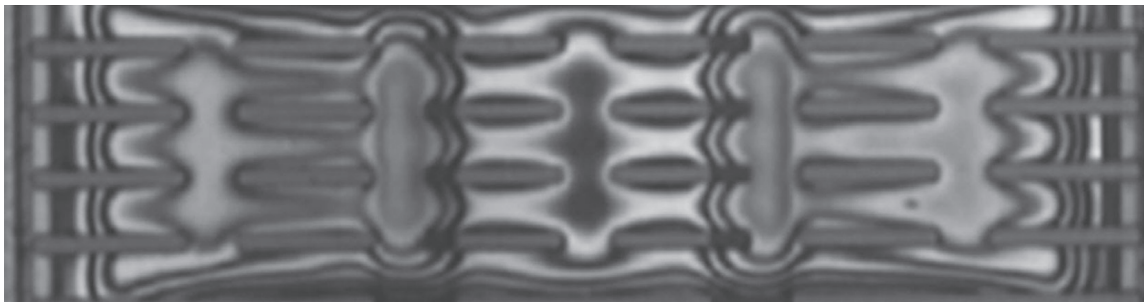

(b)

FIGURE 10.20
Image of fringes on engineering part taken using 10× interferometric objective through the 300 μm thick glass (a) without and (b) with glass compensation in reference arm of the objective.

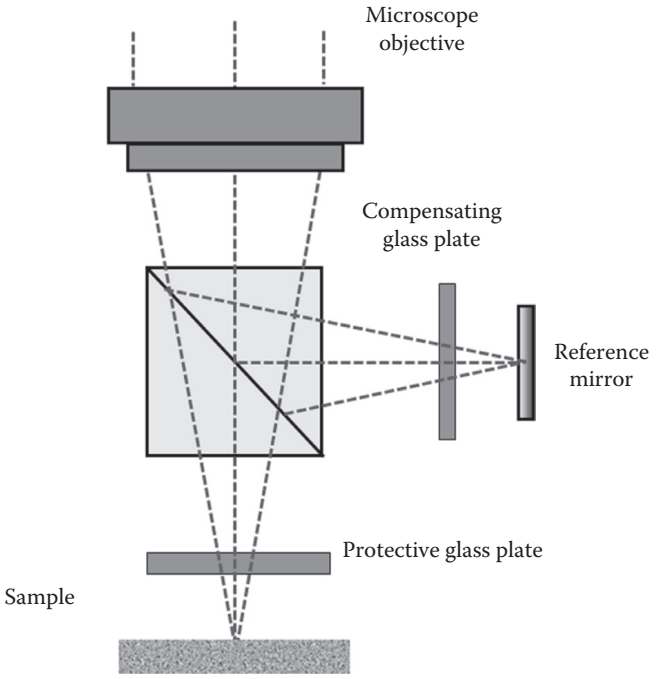

FIGURE 10.21
Michelson-type objective with a compensation plate for a measurement through the protective glass.

The effects of glass thicknesses up to 3 mm can be easily compensated for; however, for larger numerical apertures, the compensating glass thickness has to match the properties and thickness of the cover glass more precisely. Using a spectral bandwidth that is narrower than a white-light spectrum will result in better fringe contrast, and it may loosen the tolerance for incongruencies between the cover glass and the compensation glass but may be at the expense of some loss of resolution by a few nanometers.

Further improvements in thick film and through the glass measurements can be achieved by using specialized collimated illumination (see Figure 10.22) (Han and Novak 2008). This type of illumination also helps measure deep structures on a sample as shown in Figure 10.22 as well biological cells and their mechanical properties (Reed et al. 2008a,b).

10.6 3D Microscopes Based on Interference: Nomenclature

3D microscopes based on white-light interferometry may go by different names in the literature and between producers. Here is an alphabetical list of names that the reader may find. The names with their acronyms in parenthesis are most commonly used. ISO standards documents, when approved, will refer to this method as coherence scanning interferometry (CSI):

Broad-bandwidth interferometry

Coherence correlation interferometry

Coherence probe microscopy

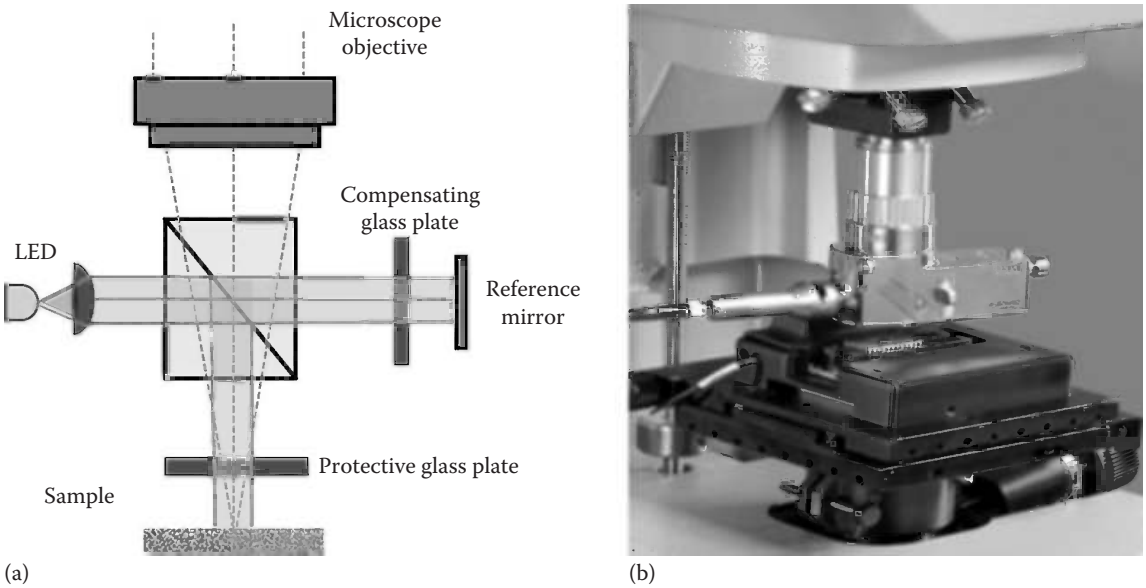

FIGURE 10.22
Michelson-type objective with a compensation plate for a measurement through the protective glass and with patented collimated illumination (shaded path) provided from under the objective for better sample penetration (a) diagram (b) photo of objective.

Coherence radar
Coherence scanning microscopy
Coherence scanning interferometry (CSI)
Mirau correlation microscopy
Fringe peak scanning interferometry
Height scanning interferometry
Interference microscope
Low coherence interferometry (LCI)
Microscopic interferometry
Optical coherence profilometry
Optical coherence microscopy
Phase correlation microscopy
Rough surface tester
Scanning white-light interferometer (SWLI)
White-light interference 3D microscope
White-light interferometry (WLI)
Vertical scanning interferometry (VSI)
White-light scanning interferometry (WLSI)
Wideband interferometry

The equivalent method for biological samples is called optical coherence tomography (OCT) but also can be called time domain OCT (TD-OCT), coherence radar, or confocal

interference microscopy. This method is mainly used with near infrared illumination for better sample penetration, and point by point scanning is used. However, in some cases, systems based on full-field, white-light microscopy are used and are called full-field or wide-field OCT systems.

10.7 Summary

WLI 3D microscopy over the last two decades has become an indispensible tool both in research labs and on production floors. The exacting specifications of many high-tech products require the ability to see, sometimes on a nanometer scale, object shape and roughness. WLI 3D microscopes provide rapid, noncontact measurements with high repeatability, reproducibility, and system to system correlation; these factors facilitate excellent production-floor throughput and quality. The systems are easy to use and deliver precise measurements for a wide range of samples that require lateral resolution on the order of microns.

For larger objects, the WLI 3D microscope even has an alternate platform design to accommodate these large-scale measurements. Finally, the rather small measured area inherent to all microscopes can be extended by taking multiple overlapping measurements and stitching images together. However, if a measurement does not include roughness, small features, or high local slopes, then other methods that are not based on the microscope setup could be considered; alternate methods should shorten measurement time, but nanometer level vertical resolution will be sacrificed; look for resolutions at hundreds of nanometers or microns.

Acknowledgment

Thank you to Bruker Nano Surfaces Division for providing many of the pictures for this chapter.

References

Ai, C. and E. Novak, Centroid approach for estimation modulation peak in broad-bandwidth interferometry, U.S. Patent 5,633,715 (1997).

Born, M. and E. Wolf, *Principles of Optics: Electromagnetic Theory of Propagation, Interference and Diffraction of Light*, Cambridge University Press, Cambridge, U.K., p. 415 (1975).

Caber, P.J., Interferometric profiler for rough surfaces, *Appl. Opt*., 32, 3438 (1993).

Danielson, B.L. and C.Y. Boisrobert, Absolute optical ranging using low coherence interferometry, *Appl. Opt*., 30, 2975 (1991).

Deck, L. and P. de Groot, High-speed noncontact profiler based on scanning white-light interferometry, *Appl. Opt*., 33(31), 7334–7338 (1994).

Doi, T., K. Toyoda, and Y. Tanimura, Effects of phase changes on reflection and their wavelength dependence in optical profilometry, *Appl. Opt*., 36(28), 7157 (1997).

Dresdel, T., G. Hausler, and H. Venzke, Three dimensional sensing of rough surfaces by coherence radar, *Appl. Opt*., 31(7), 919–925 (1992).
de Groot, P. and L. Deck, Surface profiling by analysis of white light interferograms in the spatial frequency domain, *J. Mod. Opt*., 42, 389–401 (1995).
de Groot, P. and X.C. de Lega, Signal modeling for low coherence height-scanning interference microscopy, *Appl. Opt*., 43(25), 4821 (2004).
de Groot, P. and X.C. de Lega, Interpreting interferometric height measurements using the instrument transfer function, *Proc. FRINGE 2005*, Osten, W. Ed., pp. 30–37, Springer Verlag, Berlin, Germany (2006).
de Groot, P., X.C. de Lega, J. Kramer et al., Determination of fringe order in white light interference microscopy, *Appl. Opt*., 41(22), 4571–4578 (2002).
Han, S. and E. Novak, Profilometry through dispersive medium using collimated light with compensating optics, U.S. Patent 7,375,821, May 20 (2008).
Harasaki, A., J. Schmit, and J.C. Wyant, Improved vertical scanning interferometry, *Appl. Opt*., 39(13), 2107–2115 (2000).
Harasaki, A., J. Schmit, and J.C. Wyant, Offset envelope position due to phase change on reflection, *Appl. Opt*., 40, 2102–2106 (2001).
ISO 25178-604, Geometrical product specification (GPS)—Surface texture: Areal- part 604: Nominal characteristics of non-contact in (coherence scanning interferometry), instruments, International Organization for Standardization (2012). http://www.iso.org/iso/home/store/catalogue-tc
Kino, G.S. and S.S.C. Chim, The Mirau correlation microscope, *Appl. Opt*., 29(26), 3775–3783 (1990).
Larkin, K.G., Efficient nonlinear algorithm for envelope detection in white light interferometry, *J. Opt. Soc. Am. A*, 13(4), 832–842 (1996).
Novak, E. and F. Munteanu, Application Note #548, AcuityXR technology significantly enhances lateral resolution of white-light optical profilers, http://www.bruker-axs.com/optical_and_stylus_profiler_application_notes.html (2011). (Last accessed on october 20, 2012).
Olszak, A.G. and J. Schmit, High stability white light interferometry with reference signal for real time correction of scanning errors, *Opt. Eng*., 42(1), 54–59 (2003).
Park, M.-C. and S.-W. Kim, Direct quadratic polynomial fitting for fringe peak detection of white light scanning interferograms, *Opt. Eng*., 39, 952–959 (2000).
Park, M.-C. and S.-W. Kim, Compensation of phase change on reflection in white-light interferometry for step height measurement, *Opt. Lett*., 26(7), 420–422 (2001).
Reed, J., M. Frank, J. Troke, J. Schmit, S. Han, M. Teitell, and J.K. Gimzewski, High-throughput cell nano-mechanics with mechanical imaging interferometry, *Nanotechnology*, 19, 235101 (2008a).
Reed, J., J.J. Troke, J. Schmit, S. Han, M. Teitell, and J.K. Gimzewski, Live cell interferometry reveals cellular dynamism during force propagation, *ACS Nano*, 2, 841–846 (2008b).
Schmit, J., High speed measurements using optical profiler, *Proc. SPIE*, 5144, 46–56 (2003).
Schmit, J., K. Creath, and J.C. Wyant, Surface profilers, multiple wavelength and white light interferometry, in *Optical Shop Testing*, Malacara, D. Ed., 3rd edn., Chapter 15, pp. 667–755, John Wiley & Sons, Inc., Hoboken, NJ (2007).
Schreiber, H. and J.H. Bruning, Phase shifting interferometry, in *Optical Shop Testing*, Malacara, D. Ed., 3rd edn., Chapter 14, pp. 547–666, John Wiley & Sons, Inc., New York (2007).